ARTICLES

Performance Analysis of Air-to-Water Heat Pump Systems Using R290 Refrigerant Adapted to Nordic Climates

Key words: Air-to-water heat pump; Propane as refrigerant; Field test; Performance modelling; Defrost operation; Nordic climate applications



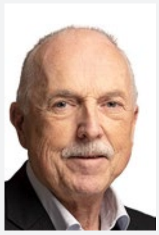

JAE-HEE LEE[a] SIMWON CHIN[b] TRYGVE MAGNE EIKEVIK[c]

[a] Department of Built Environment, Oslo Metropolitan University, Norway
[b] LG Electronics Inc., Seoul, Republic of Korea
[c] Department of Energy and Process Engineering, Norwegian University of Science and Technology, Trondheim, Norway

[a] Co-authors: Peter Geoffrey Schild, Moon Keun Kim[1]
[a,1] Corresponding author: Moon Keun Kim (E-mail address: Moon.Kim@oslomet.no)
[b] Co-authors: Donghan Kim, Dongkeun Yang, Beomsoo Seo

Air-to-water heat pumps (AWHPs) with propane (R290) as working fluid have gained attention as efficient and environmentally friendly space heating solutions. This study conducts field tests and analyzes the performance of an R290 AWHP heating system during winter operation in Oslo, Norway. Field observations demonstrate effective defrost operations, resulting in reliable heating performance and high energy efficiency under cold and humid outdoor conditions. A field-measurement-based model is developed to evaluate seasonal performance of R290 AWHP systems under Nordic climate conditions, providing valuable reference data for their application in one of the most challenging environments for heat pump operation.

The importance of adopting high-efficiency heating systems, such as air-to-water heat pumps (AWHP), is growing in Europe, as heating-related energy consumption accounts for a significant portion of building energy use [1]. However, their widespread adoption has raised environmental concerns due to the use of fluorinated refrigerants, including HFCs and HFOs. Accordingly, the use of alternative refrigerants, including propane (R290) heat pumps, has been highlighted due to a low global warming potential of 3, high efficiency, and wide operating temperature range suitable for space heating in cold climates [2].

In cold regions, especially Nordic climates characterized by low temperatures and high humidity in winter, AWHP performance degradation, primarily due to frost accumulation, remains a critical issue requiring attention [3]. Frost accumulation on the outdoor-coil fins diminishes heat exchange efficiency and increases compressor pressure ratio, ultimately leading to abnormal heating operation and low energy efficiency [4]. Although these issues may similarly arise in R290 AWHP operations, limited case studies are available on their performance analysis under such cold and humid climatic conditions.

In this study, an R290 AWHP system was installed in an occupied building in Oslo, Norway, to investigate its defrost operation, heating performance, and energy efficiency during winter. Subsequently, system performance over the entire heating season under Nordic climate conditions was predicted using data-driven modelling based on field measurements. This study would contribute to proactively examining operational characteristics under real-ambient conditions and predicting overall performance adapted to Nordic climates, prior to the widespread adoption of R290 AWHP systems.

Field Test Overview

System description

Figure 1 illustrates the system configuration, including the installation layout within the building at the Oslo test site. The outdoor AWHP, supplied by LG Electronics, utilizes R290 refrigerant. A mixture of 30% ethylene glycol and 70% water is used as the heat transfer medium between the AWHP and the plate heat exchanger, to prevent freezing during the winter heating season. The hot fluid mixture from the AWHP transfers heat to the water circulating through a buffer tank via a plate-type heat exchanger until the target water temperature is reached. The heated water stored in the buffer tank in the first-floor mechanical room is distributed to radiators in each zone on every floor. Detailed specifications of the AWHP are listed in **Table 1**.

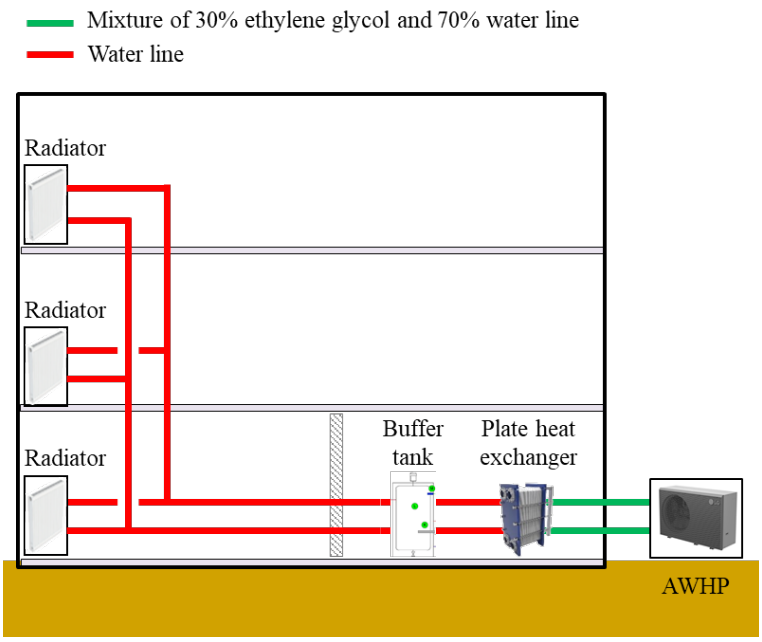

Figure 1. Schematic diagram of the R290 AWHP system installed at the Oslo site.

Table 1. *Specifications of the AWHP.*

Parameters	Outdoor dry-bulb temperature	Leaving water temperature	Values
Heating capacity	7°C	35°C	12.0 kW
		55°C	10.0 kW
	2°C	35°C	12.0 kW
	-7°C	35°C	11.8 kW
		55°C	9.3 kW
Water flow rate (Rated at 5°C temperature difference)			34.5 ℓ/min
Refrigerant type			R290

Note:
1. Performance are in accordance with EN14511 and reflect ErP testing conditions.
2. Measuring procedure follows EN14511.
3. Seasonal coefficient of performance is in accordance with EN14825.

Measurements

The system was installed in a three-story office building, featuring 14.3 m × 10.3 m × 9.32 m, located near the harbor in Oslo, Norway. The system operated from January 28th to February 26th, 2025, during which the target water temperature (T_{target} [°C]) for space heating was manually set.

Operational data were collected at two-second intervals, primarily using LG Monitoring View (LGMV) software. The LGMV software also recorded the system defrost mode (0: inactive, 1: active), and webcam footage was additionally used to monitor frosting and defrosting of the outdoor coil. Outdoor relative humidity was not directly measured and instead substituted with data from a nearby observation site [5].

The heat output from the AWHP ($\dot{Q}$ [kW]) was calculated by multiplying the thermal capacitance of the mixture $(\dot{m}{\cdot}c_p)_{mix}$: $\dot{m}$ [kg/s], c_p [kJ/kg K]) by the temperature difference between the condenser outlet.

($T_{cond,o,mix}$ [°C]) and inlet (($T_{cond,i,mix}$ [°C]), as shown in Equation (1). The input power ($\dot{P}$ [kW]) includes the power consumed by all components, encompassing the compressor, outdoor fan, pump circulating through the plate-type heat exchanger, and controller. The coefficient of performance (COP [W/W]) was calculated by dividing $\dot{Q}$ by $\dot{P}$, using Equation (2).

$$\dot{Q} = (\dot{m} \cdot c_p)_{mix} \times (T_{cond,o,mix} - T_{cond,i,mix}) \quad (1)$$

$$COP = \dot{Q}/\dot{P} \quad (2)$$

The seasonal performance factor (SPF) was defined as the average performance of a heat pump during a year or the heating season. A previous report [6] categorized SPF by system boundary, and this study adopted SPF-H2, which calculates SPF within the H2 boundary. This boundary includes the heat pump unit and auxiliary equipment supplying the heat source (e.g., fans and pumps), while excluding the backup heating system, buffer tank immersion, and building-side distribution equipment. Accordingly, SPF-H2 was calculated as the ratio of cumulative heat output (Q) to cumulative input power (P) within the H2 boundary over the field-test periods, with units of kWh/kWh, as shown in Equation (3).

$$SPF = \sum Q / \sum P \quad (3)$$

Field Performance Analysis

Defrost operation

Figure 2 presents a scatter plot of outdoor dry-bulb temperature (T_{oa} [°C]) versus relative humidity (RH_{oa} [%]) under conditions in which defrost operations were observed during field testing. The colour bar indicates the duration of each defrost event. The average duration of all observed defrost operations was estimated at 5.10 minutes, with durations ranging approximately from 2 to 8 minutes. Notably, defrost durations were actively controlled and strongly affected by RH_{oa}, more than by T_{oa}, increasing with higher RH_{oa}, which favours frost formation and growth. The observed outdoor condition range and corresponding defrost durations will be used for defrosting modelling and performance prediction in Nordic climates in the following sections.

Figure 3 illustrates detailed defrost performance observed during field testing. **Figure 3(a)** presents webcam footage captured during the defrost process, highlighting that defrost operations thoroughly removed frost from the coil, with no cumulative freezing observed upon completion. **Figure 3(b)** shows the duration of each subsequent post-defrost heating operation, categorized by defrost-cycle interval. The defrost-cycle interval is defined as the time between the end of one defrost cycle and the start of the next. Throughout the field tests, a consistent post-defrost heating duration was maintained for each defrost-cycle interval. Specifically, even when defrost operations occurred frequently at intervals of less than one hour, the post-defrost heating duration remained stable at approximately 40 minutes, without any reduction. As the interval between defrost operations increased, the duration of the subsequent heating operation also extended, effectively filling the longer

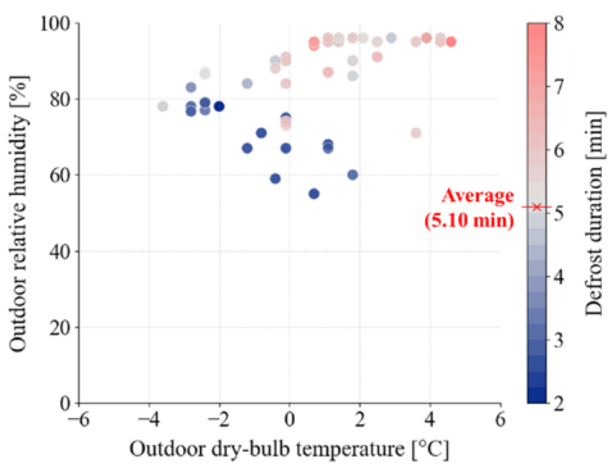

Figure 2. Outdoor conditions during defrost operations with observed durations from field tests.

gap with continuous heating. Therefore, space heating was reliably maintained after defrosting, with no interruptions or insufficiencies observed across all defrost-cycle intervals. These results highlight that the defrost operations of the system were successful, as neither cumulative frost accumulation nor abnormal heating operation due to defrosting was detected.

The outdoor conditions during each post-defrost heating phase, also categorized by defrost-cycle interval, indicate that the intervals were adaptively controlled in response to outdoor conditions, rather than governed by a fixed-time periodic logic. Higher outdoor humidity tended to shorten the defrost-cycle interval, leading to more frequent defrost operations. Additionally, at similar humidity levels, lower outdoor temperatures led to shorter intervals as well. This outdoor-environment-adaptive control enabled the system to achieve high-performance defrost operation and maintain reliable heating throughout the field tests.

(a) Webcam footage during defrost operation

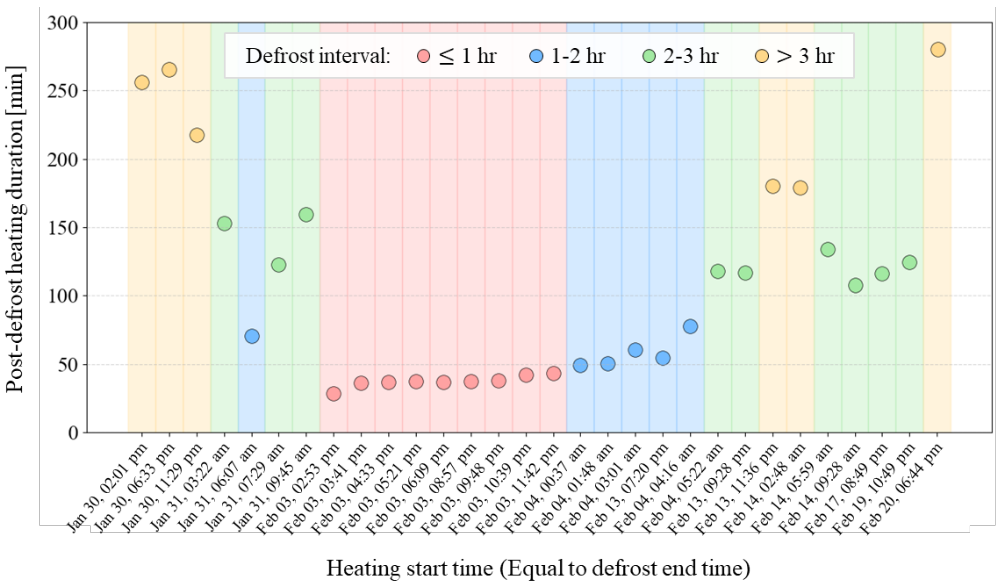

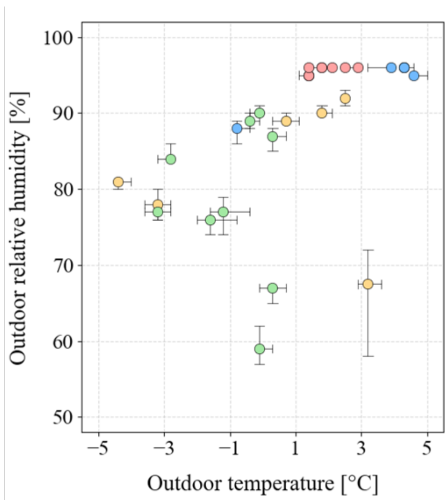

Outdoor condition distribution during each post-defrost heating operation

(b) Post-defrost heating duration for each defrost-cycle interval

Figure 3. Defrost performance.

Heat output and energy efficiency

Figure 4 presents time-series graphs of the measured $\dot{Q}$ and COP at a T_{target} setting of 50°C, reflecting typical Norwegian space heating water setpoint practices, along with corresponding outdoor condition variations. The results include only normal heating operation, excluding defrost phases, to highlight the fundamental heating performance. $\dot{Q}$ tends to increase when T_{oa} decreases and RH_{oa} increases, indicating rising heating demand and system operation approaching full load. COP tends to decrease as T_{oa} decreases and RH_{oa} increases, due to an increased compressor pressure-ratio and reduced heat exchanger efficiency. For reference, the system operates in a reverse refrigeration cycle during defrosting (i.e., cooling cycle), during which $\dot{Q}$ and COP temporarily show negative values.

Figure 5 presents improvements in measured COP values at a T_{target} of 50°C, compared to the rated values at each standard T_{oa} specified in the manufacturer product data book (PDB). The rated values at T_{target} of 50°C were estimated by curve fitting relevant data provided in the manufacturer PDB, and these fitted values were then used to calculate the COP improvements. COP improvements exceeding 100% accounted for approximately 97% of all cases; in other words, nearly all measured COP values outperformed the PDB rated values, validating the quality of field measurements. All average COP improvements at each standard T_{oa} also exceeded 100%.

Over the field-test periods at a T_{target} setting of 50°C, a total SPF-H2 of 3.21 was obtained considering the use of a 30% ethylene glycol and 70% water mixture. Although differences in the defined system boundaries preclude a strictly fair comparison, the present study exhibits a 39.6% improvement in SPF relative to the previous field study conducted in Norway [7], due to the more efficient AWHP operation adapted to Nordic climates.

For reference, excluding defrost phases yielded an SPF-H2 of 3.24 with the ethylene glycol-water mixture conditions. The insignificant difference from the total SPF-H2 is likely due to effective outdoor-adaptive defrost control, combined with the low frequency of defrost events during field testing, associated with unexpectedly mild weather.

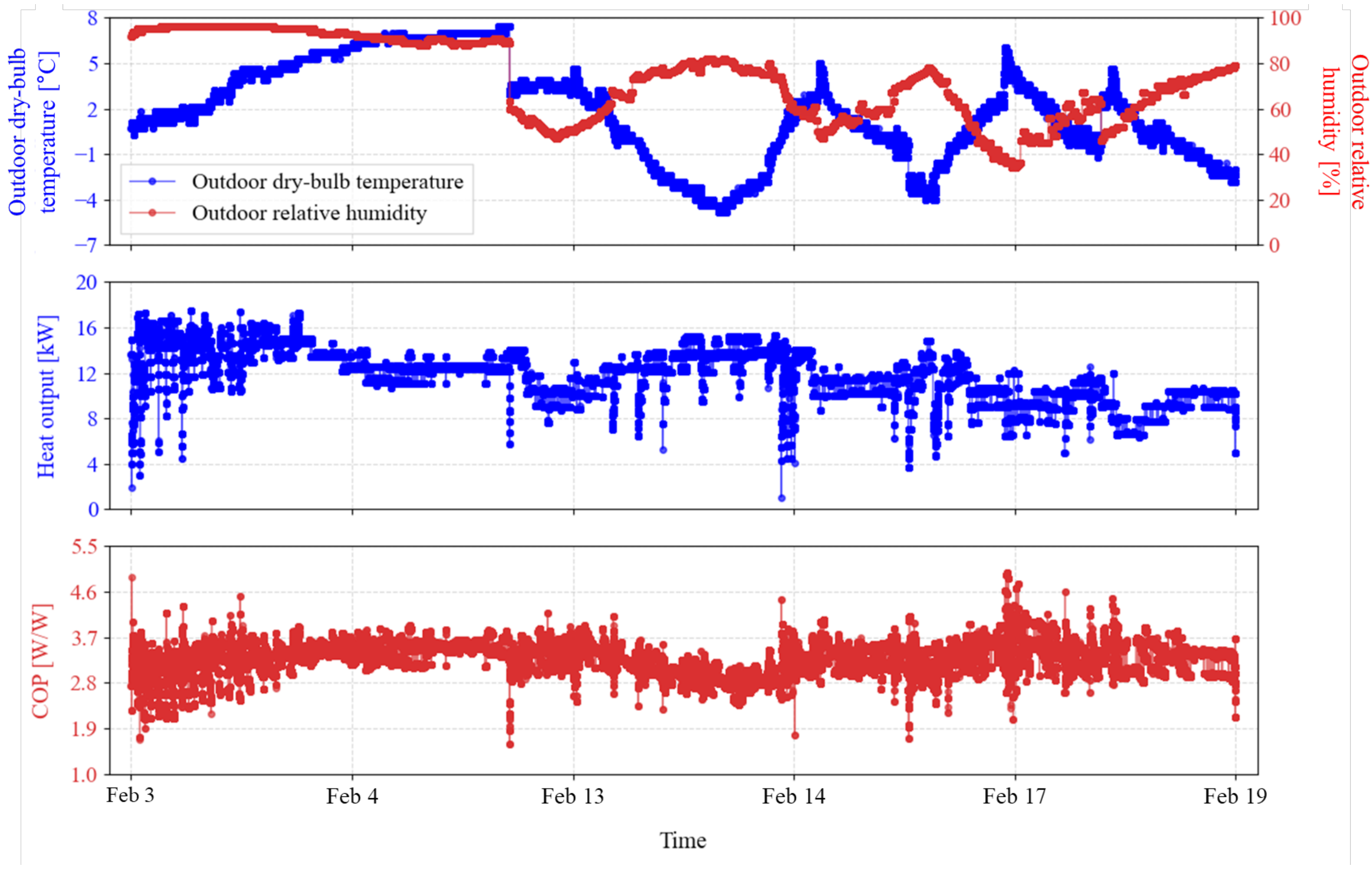

Figure 4. Heat output and COP at target water temperature of 50°C along with outdoor condition variations during field tests.

Performance Modelling

To investigate system performance across the full range of Nordic climates, performance modelling was conducted using field-test data, explicitly incorporating defrost operations.

Defrost code

The defrost code ($C_{defrost}$ [-]), a binary variable indicating defrost operation (0: inactive, 1: active), was modelled based on T_{oa}, RH_{oa}, outdoor dew-point temperature (DP_{oa} [°C]), and refrigerant temperature in the evaporator (T_{evap} [°C]), in conjunction with defrost performance, all observed in field measurements. The specific range of outdoor conditions associated with defrost mode activation was derived using these variables and incorporated into the defrost modelling.

First, the specific region in which defrost operation can potentially occur was identified on a $T_{oa} - RH_{oa}$ scatter plot. This region was delineated above several lines connecting the warmest and driest outdoor conditions observed during defrost events, as depicted in **Figure 2**. Second, a regression line representing DP_{oa} threshold for defrost mode activation was defined as a function of T_{oa} based on field measurements. Accordingly, defrost mode was activated when T_{evap} fell below the DP_{oa} value defined by the regression line, provided that the outdoor conditions also lay within the specific $T_{oa} - RH_{oa}$ region identified in the first step.

Once activated, the defrost operation was modelled to last 5 minutes, consistent with the average duration observed in field measurements. Upon completion, system performance was modelled to return to normal immediately, with no residual effects from cumulative frost accumulation.

Heat output, input power, and COP

Second-order polynomial regression models were developed for $\dot{Q}$ and $\dot{P}$, using T_{oa}, RH_{oa}, $C_{defrost}$, temperature difference between the condenser outlet and inlet (ΔT_{mix} [°C]), T_{target}, and the percentage error (Err_{target} [%]) in meeting T_{target} as input variables, yielding R-squared values of 0.9934 and 0.9218, respectively. Subsequently, COP was modelled by dividing the predicted $\dot{Q}$ by the predicted $\dot{P}$.

Predicted Performance Analysis in Nordic Climates

System performance over the Oslo heating season—January to April and October to December—was predicted using the developed models and EnergyPlus IWEC climate dataset [8]. Data points with $T_{oa} > 10$°C or $RH_{oa} < 40$%, accounting for 10% of the dataset, were infrequent during the Oslo heating season and lay significantly outside the field-test range; thus, they were excluded to avoid compromising prediction accuracy.

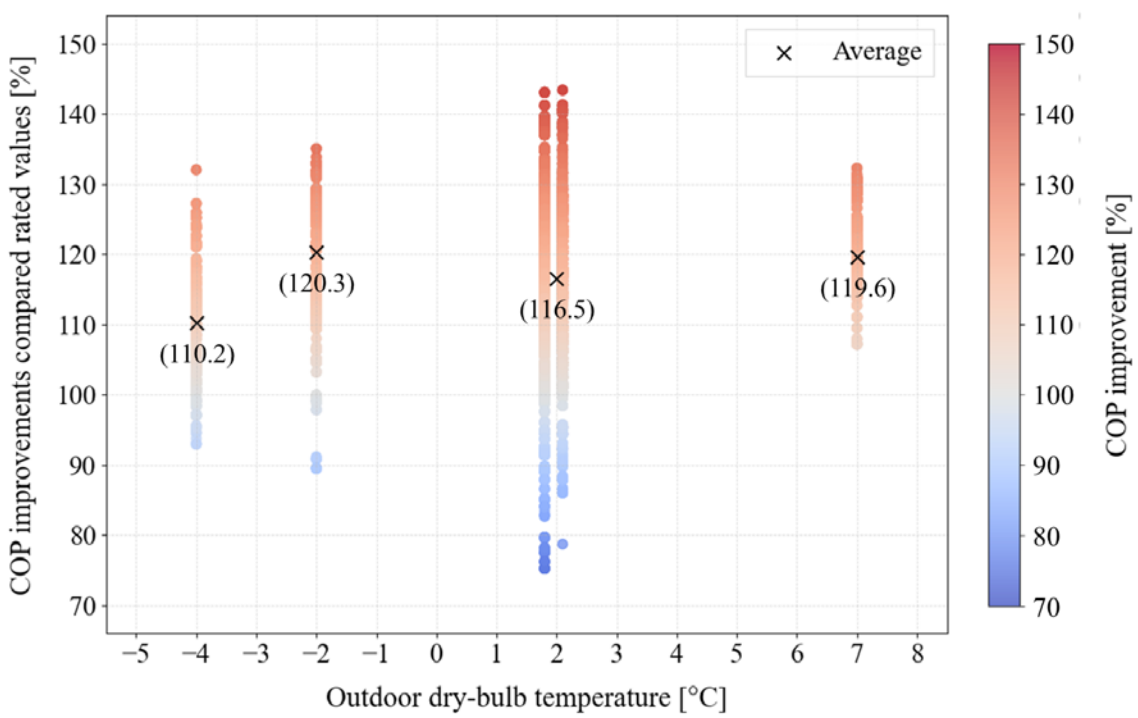

Figure 5. COP improvements compared to rated values at target water temperature of 50°C.

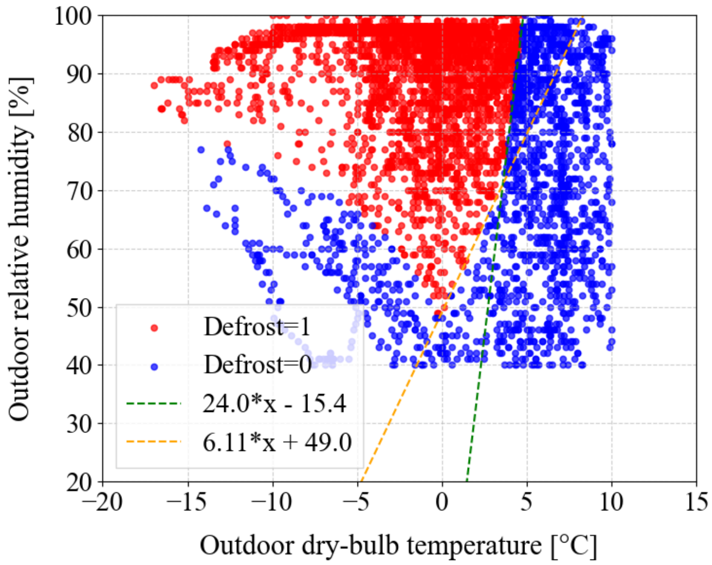

Figure 6. Defrost mode activation predicted by defrost code.

Figure 6 illustrates the predicted defrost mode on a $T_{oa} - RH_{oa}$ scatter plot across the Nordic climate range, where blue and red markers represent the inactivation ($C_{defrost} = 0$) and activation ($C_{defrost} = 1$), respectively. The defrost mode was activated under cold and humid outdoor conditions, as defined by the green and yellow boundary lines and the DP_{oa} threshold regression line, all derived from $C_{defrost}$ modelling. With the defrost duration modelled as 5 minutes, the resulting frequency of defrost operation accounted for 5.49% of the total operating period in Nordic applications.

Figure 7 presents a heat map of the predicted COP, where each cell represents the average COP for the number of data points (n) within the corresponding $T_{oa} - RH_{oa}$ interval. The average COP generally decreases with decreasing T_{oa} and increasing RH_{oa}, with notably low values observed under outdoor conditions associated with more frequent defrost mode

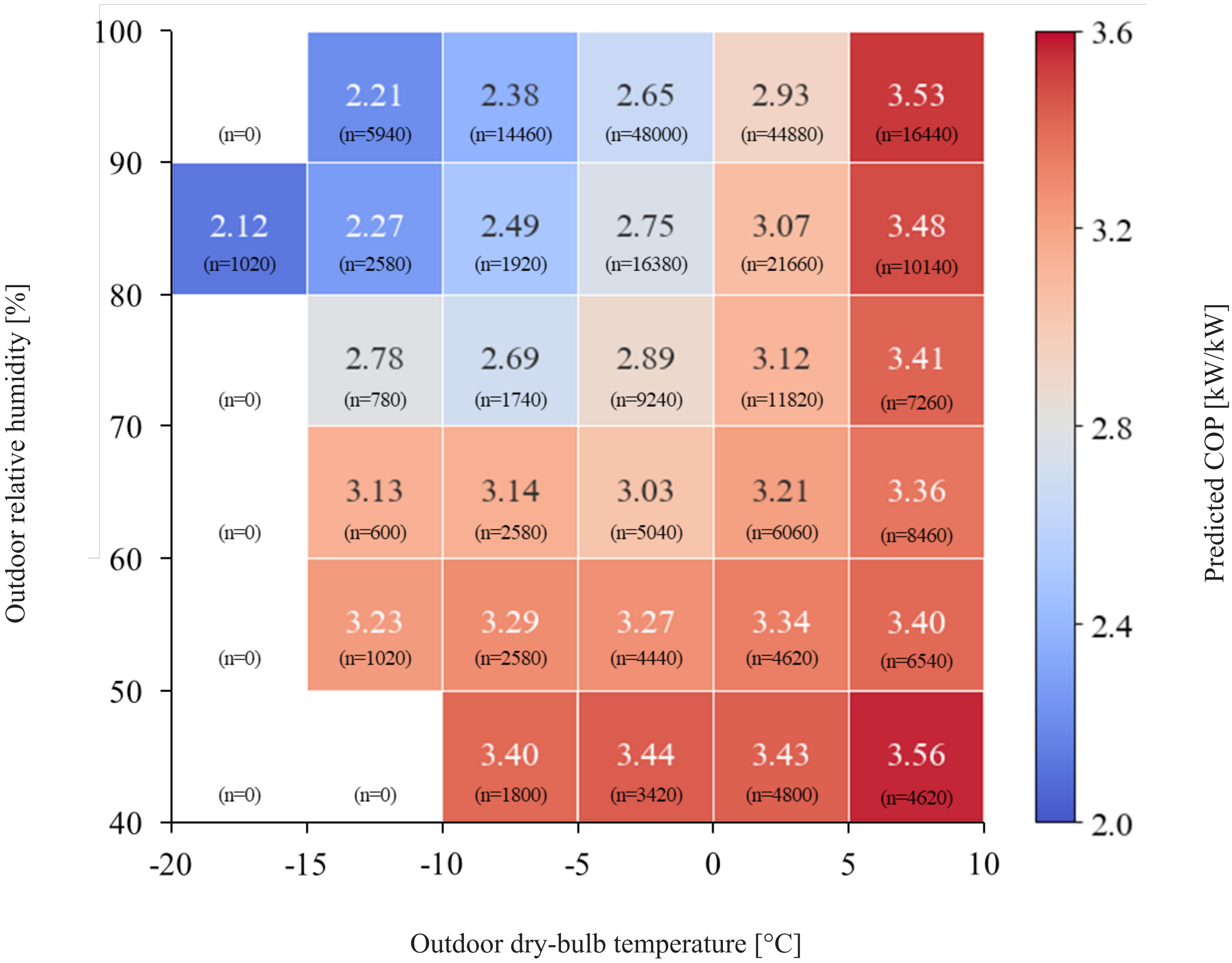

Figure 7. Heat map of predicted COP values.

activation, specifically when T_{oa} is below 0°C and RH_{oa} exceeds 70%. Consequently, SPF-H2 over the heating season in Nordic climates is predicted to be 3.04 under ethylene glycol-water mixture conditions. For reference, excluding defrost phases yields a SPF-H2 value of 3.10 with the mixture conditions.

The differences between predicted and field-measured SPF-H2 values are attributed to the inclusion of more extreme outdoor winter conditions in the predictions, adapted to Nordic climates, and the corresponding increase in defrost operation. Additionally, COP predictions inherently involve propagation errors from simulation-based estimates of both $\dot{Q}$ and $\dot{P}$, potentially leading to amplified cumulative inaccuracies – particularly under outdoor conditions that deviate significantly from those observed during field testing.

Conclusions and Future Works

This study analyzed the performance of an R290 air-to-water heat pump (AWHP) system through winter field testing in Oslo, Norway. Field measurements confirmed high-performance defrost operation under cold and humid outdoor conditions, with no frost accumulation or abnormal post-defrost heating detected. The outdoor-environment-adaptive defrost control ensured reliable heating performance and high energy efficiency throughout the tests. The seasonal performance factor across the Nordic climate range was predicted to be 3.04 using the ethylene glycol-water mixture conditions, providing a valuable reference for R290 AWHP application in Nordic climates.

However, unexpectedly mild weather conditions during field testing may have limited the observation of more extensive defrost operation and the acquisition of performance data under full-load operation. Additionally, the slightly lower COP observed in this study may be attributed to the high target water temperature setting of 50°C, the insulation characteristics of the building and system, and the inclusion of all components – particularly the fan and pump – in the power measurements.

Future work will address these limitations and empirically evaluate system performance across the full Nordic climate range. More comprehensive data will also be used to characterize frost formation patterns and defrost-cycle dynamics in greater detail. Upon fully confirming system feasibility, further analysis will examine the impact of using R290 relative to alternative refrigerants and its applicability in other European regions. Moreover, performance of multiple R290 AWHPs on the water/glycol side will be explored under various cascade operation scenarios—such as concurrent parallel or alternating operation—along with the optimization of the associated control logic.

References

[1] IEA (2023), Tracking Clean Energy Progress 2023, IEA, Paris https://www.iea.org/reports/tracking-clean-energy-progress-2023, Licence: CC BY 4.0.

[2] Zou, L., Liu, Y., & Yu, J. (2024). Recent advances on performance enhancement of propane heat pump for water heating applications. Energy, 134251.

[3] Gibb, D., Rosenow, J., Lowes, R., & Hewitt, N. J. (2023). Coming in from the cold: Heat pump efficiency at low temperatures. Joule, 7(9), 1939-1942.

[4] Song, M., & Deng, S. (2019). Defrosting for Air Source Heat Pump: Research, Analysis and Methods. Woodhead Publishing.

[5] Norwegian Centre for Climate Services, Observations and weather statistics. Available from: https://seklima.met.no/observations/.

[6] Nordman, R., Kleefkens, O., Riviere, P., Nowak, T., Zottl, A., Arzano-Daurelle, C., Lehmann, A., Polyzou, O., Karytsas, K., Riederer, P. et al. SEasonal PErformance Factor and MOnitoring for Heat Pump Systems in the Building Sector (SEPEMO-Build). Final Report, SP Technical Research Institute of Sweden: Borås, Sweden, 2012.

[7] Stignor, C. H., & Walfridson, T. (2019). Nordsyn study on air-to-water heat pumps in humid Nordic climate. Nordic Council of Ministers.

[8] EnergyPlus, Weather Data. Available from: https://energyplus.net/weather. ■